Journal of Sohag Agriscience (JSAS) 2025, 10(2): 100-113

ISSN 2735-5578
https://jsasj.journals.ekb.eg
JSAS 2025; 10(2): 100-113

Received: 25-08-2025
Accepted: 31 -08-2025

Abdelrahman A. Mustafa
Ali R. A. Moursy
Osama K. Ahmed
Soil and Water Department
Faculty of Agriculture
Sohag University
Sohag
8254
Egypt

Mohamed E. Fadl
Division of Scientific Training and Continuous Studies
National Authority for Remote Sensing and Space Sciences (NARSS)
Cairo
11769
Egypt

Corresponding author:
Abdelrahman A. Mustafa
a_mustafa32@yahoo.com

Characterization of Some Sohag Soils Using Traditional and Advanced remote sensing techniques

Abdelrahman A. Mustafa, Mohamed E. Fadl, Ali R. A. Moursy and Osama K. Ahmed

Abstract

This study evaluated the soils of Sohag Governorate, Egypt, using both traditional laboratory analysis and vis-NIR spectral data from 140 surface soil samples. Laboratory results showed wide variability in key soil properties whereas calcium carbonate ($CaCO_3$) ranged from 0.76% to 34.60% with a mean of 5.82%, cation exchange capacity (CEC) varied from 1.44 to 32.38 cmol(+)/kg with an average of 9.22 cmol(+)/kg, clay content ranged from 1.59% to 54.76% (mean 16.79%), and electrical conductivity (ECe) spanned from 0.38 to 30.24 dS/m (mean 4.82 dS/m). High sample variances were recorded, particularly for clay (104.66), reflecting spatial and land use diversity across old and newly reclaimed soils. Correlation analysis among these properties revealed a moderate positive correlation between $CaCO_3$ and CEC ($r = 0.52$), and weaker negative correlations between $CaCO_3$ and both clay ($r = –0.25$) and EC ($r = –0.30$), while clay showed a positive association with EC ($r = 0.34$). Spectral data collected in the 350–2500 nm range revealed distinctive spectral behaviors for each property. Soils with high $CaCO_3$ content exhibited increased reflectance, especially in the 2200–2350 nm region, where negative correlations reached $r < –0.60$. CEC showed a positive correlation with reflectance, notably around 2100–2250 nm (up to $r = +0.60$), due to associations with OH-bearing clay minerals. Clay content had the strongest spectral signal, with positive correlations exceeding +0.70 in the 2100–2300 nm range, while EC was moderately and positively correlated ($r \approx +0.40$ to $+0.50$) with reflectance near 1450 nm, 1950 nm, and 2200 nm. These results confirm that the shortwave infrared region (SWIR) is particularly sensitive to variations in soil composition. The integration of vis-NIR spectroscopy with traditional methods demonstrated the feasibility of rapid, non-destructive soil characterization. The spectral approach, while dependent on calibration with laboratory data, offers significant time and cost savings for large-scale assessments. This study emphasizes the complementary value of combining conventional and spectral techniques for efficient monitoring and management of heterogeneous soils, particularly in arid and semi-arid landscapes like Sohag. The identification of key spectral bands for each property paves the way for predictive modeling and digital soil mapping, contributing to precision agriculture and sustainable land use planning.

Key words: Sohag soils, vis-NIR spectroscopy, soil property variability, spectral correlation analysis, remote sensing in agriculture

INTRODUCTION

The characterization of soil properties is a critical component of sustainable land management and precision agriculture, as it directly influences crop productivity, resource utilization, and environmental stewardship (Moursy et al., 2020; Nungula et al., 2024). Traditional approaches to soil characterization have relied heavily on field surveying, systematic sampling, and laboratory analysis to assess key soil parameters such as electrical conductivity (EC), cation exchange capacity (CEC), clay content, and calcium carbonate ($CaCO_3$) as described in several studies such as El-Sayed et al. (2023) and Shokr et al. (2024). Field surveying provides the spatial context and ensures representative sampling, while laboratory analyses using wet-chemistry methods yield accurate measurements of soil attributes (Mustafa & Moursy 2020a; Moursy et al., 2022). However, these conventional methods are often labor-intensive, time-consuming, and costly, especially when large areas or high sample densities are required for detailed soil mapping and monitoring (Mustafa & Moursy 2020b; Abd-Elazem et al., 2024). The logistical challenges associated with collecting, processing, and analyzing numerous soil samples can significantly hinder the timely acquisition of essential soil information needed for effective decision-making in agricultural and environmental management (AbdelRahman et al., 2025; Moursy, 2025). In recent years, the integration of soil spectral data with traditional field surveying and sampling has emerged as a promising solution to overcome the limitations of conventional soil analysis (Shokr et al., 2024; Mondal et al., 2025). Soil spectral data, particularly those obtained from visible and near-infrared (Vis-NIR) hyperspectral reflectance spectroscopy; offer a rapid, non-destructive, and cost-effective means of assessing multiple soil properties simultaneously (Mustafa & Moursy 2020b; Wang et al., 2024). By capturing the unique spectral signatures associated with different soil constituents, hyperspectral data enable the estimation of EC, CEC, clay content, and $CaCO_3$ with a high degree of accuracy when calibrated against reference laboratory measurements (El-Sayed et al., 2023). The process typically involves collecting soil samples through systematic field surveys, analyzing a subset of these samples in the laboratory to establish ground-truth values, and then using spectral reflectance measurements to develop predictive models. These models, often enhanced by machine learning algorithms, can then be applied to spectral data from additional samples or even in situ field measurements, facilitating the rapid characterization of soil properties across larger spatial extents (AbdelRahman et al., 2025; Abd-Elazem et al., 2024; Moursy et al., 2025). The synergy between field surveying, sampling, and spectral analysis is particularly valuable for mapping the spatial variability of soil properties, which is essential for precision agriculture and land resource management (Mustafa & Moursy 2022; Mondal et al., 2024). Field surveys ensure that sampling captures the inherent heterogeneity of the landscape, while laboratory analyses provide the reference data needed to calibrate and validate spectral models (Shokr et al., 2024; Mondal et al., 2025). Once robust relationships between spectral features and soil properties are established, spectral data can be used to generate high-resolution maps of EC, CEC, clay, and $CaCO_3$, supporting site-specific management practices and more efficient allocation of agricultural inputs. This integrated approach not only reduces the time and cost associated with traditional soil analysis but also minimizes environmental impacts by decreasing the reliance on chemical reagents and extensive laboratory work (Moursy, 2025). Moreover, the use of soil spectral data in conjunction with field surveying and sampling enhances the scalability and repeatability of soil characterization efforts (Mondal et al., 2025). Hyperspectral sensors, whether deployed in the laboratory, field, or mounted on airborne or satellite platforms, can rapidly acquire large volumes of data, enabling frequent monitoring of soil conditions over time (Shokr et al., 2024; Thabit & Moursy 2024). This capability is crucial for detecting changes in soil properties due to land use, management interventions, or environmental factors (Wang et al., 2024). The integration of spectral data with geospatial technologies further facilitates the analysis and visualization of soil variability, supporting informed decision-making at multiple scales. Therefore, the objectives of this study are (i) to characterize some Sohag soils using traditional methods; (ii) to characterize the soils using the vis-NIR spectral signatures; and (iii) to compare the two techniques and recommend the optimal one.

MATERIALS AND METHODS

The figure (1) showed the employed materials and methods in this study. Soil surveying, sampling, preparation and testing were conducted as well as the soil spectral signatures were acquired. Mathematical and statistical calculations were done using R studio software to address the relation between the soil properties and the spectral data.

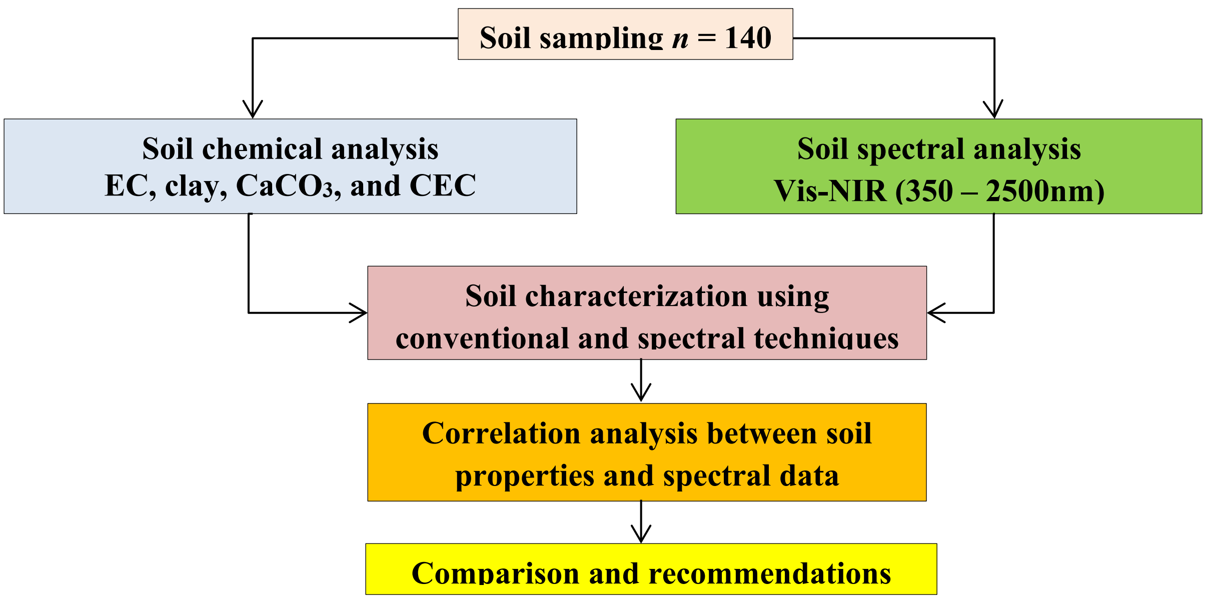

Figure (1). Employed materials and methods in the study.

Study area

The study area (figure 2) is situated in Sohag Governorate, Egypt, covering a stretch of the Nile Valley from the northern edge of Qena Governorate to the southern edge of Assiut Governorate, between longitudes 31°20′ and 32°14′ E. This region spans 11,022 km², with the Nile River running for 125 km and the valley width ranging from 16 to 20 km, plus a desert hinterland extending about 90 km eastward. Only about 15% of the governorate's area is inhabited, which is equivalent to 2.07% of Egypt's total area (Mustafa, 2023). Land use and land cover in the area are diverse: cultivated lands dominate at 60.7% of the total geographic area, followed by desert lands (23.6%), urban areas (12.3%), and water bodies (3.4%) as studied by Mustafa (2023). The cultivated lands include both old Nile Valley fields and lands under reclamation, while urban and rural settlements, services, commercial, and industrial areas make up a significant portion of the land. Sohag province is administratively divided into 12 central units, 10 cities, 51 local units, 270 mother villages, and 1,217 small villages (Mustafa & Negim, 2016). The population is projected to reach nearly 5.9 million in 2025, with 78% living in rural areas (CAPMAS, 2025). Geologically, the area is shaped by the Nile's alluvial deposits, which create fertile soils along its banks, consisting of silt, clay, and sand transported from the Ethiopian Highlands. To the east, the landscape transitions into the arid Eastern Desert, marked by ancient sandstone formations, while the Western Desert features sand dunes, limestone plateaus, and sedimentary rock outcrops. Fossil evidence in limestone and clay hints at ancient marine environments. The terrain varies from 100 to 300 meters above sea level and is underlain by several groundwater aquifers, the most productive of which are composed of sand, gravel, and clay lenses, with groundwater generally flowing eastward towards the Nile (Embaby et al., 2023). Hydrologically, groundwater is the second most important water source in Sohag after the Nile, serving agricultural, domestic, and industrial needs (Ahmed & Ali, 2011). The governorate manages a network of government and local wells, with six main production wells serving 8,100 acres and 1,279 local wells benefiting 7,376 acres. Irrigation practices vary, with surface irrigation being most common, especially in newly reclaimed lands, while drip irrigation is limited to a few centers and covers a smaller area (Negim & Moursy 2023). The climate is arid, characterized by hot summers and mild winters, with average temperatures ranging from 13.9°C in January to 32.8°C in July. Relative humidity fluctuates between 33% and 61% depending on the season, and rainfall is scarce and irregular (El-Zohry et al., 2024). Agriculturally, Sohag Governorate has about 322,000 feddans of cultivated land and is known for traditional crops like wheat, onions, beans, and cotton, as well as being a major producer of sugarcane (General Authority for Inquiries, 2023). Most soils are used for field crops, with limited cultivation of vegetables and fruit trees due to the heavy, old soils that are less suitable for such crops (Ouda et al., 2016). Recent years have seen the reclamation and cultivation of new lands, particularly in the western part of Sohag, such as West Tahta and West Geheina. These efforts have expanded the agricultural base and introduced new soil management challenges and opportunities. The soils of Sohag are diverse, ranging from sand and loamy sand to clay and clay loam in cultivated areas, and from fine sand and siltstone to gravel in newly reclaimed desert lands (Ahmed, 2007). Studies have shown that soils in the region can be slightly to strongly alkaline, with variable salinity and low organic matter. For example, El-Sayed et al. (2020) and Moursy et al. (2020) found that soils in parts of Sohag have low CEC, low SOM, and $CaCO_3$ content ranging from low to very high. Soil fertility is often limited by low available micronutrients and nitrogen, though potassium levels can vary widely. The texture of soils in old cultivated lands is usually clay, sandy loam, or loam, while newly reclaimed areas may have sandy clay, clay loam, or sandy soils, often improved by the addition of alluvium. These variations reflect both the natural diversity of the landscape and the impact of human intervention in land reclamation and soil management (Mustafa, 2023).

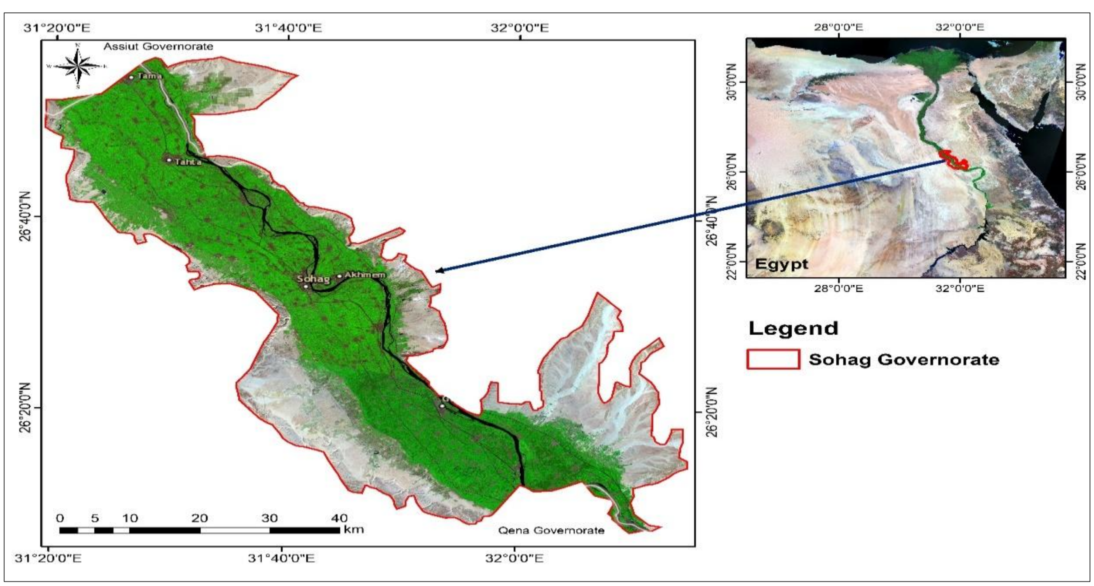

Figure (2). Location map of the study area.

Soil sampling and testing

A total of 140 surface soil samples (0–25 cm) were collected from various locations across Sohag Governorate to represent both old and newly reclaimed soils. The coordinates of each sampling site were precisely recorded using a Garmin eTrex 10 Worldwide Handheld GPS Navigator, ensuring accurate spatial referencing for subsequent analysis. After field collection, the soil samples were transported to the laboratory for preparation and chemical analysis. Samples were air-dried for two days, then crushed and sieved through a 2 mm mesh. The fraction of smaller than 2 mm was used for laboratory determinations of soil properties. Electrical conductivity (ECe) of the soil paste extract was measured with an Orion model 150 EC meter (USA). Total calcium carbonate ($CaCO_3$) content was determined volumetrically using Colins's calcimeter, following the method of Jackson (1973). Cation exchange capacity (CEC) was measured by saturating the soil with 1M sodium acetate solution (pH 8.2) and replacing with 1M ammonium acetate solution (pH 7.0). Available nitrogen, which serves as a representative metric for CEC, was determined using the micro-Kjeldahl method as described by Baruah and Barthakur (1997). Soil texture was analyzed using the hydrometer method. To prepare for texture analysis, soluble salts and soil organic matter (SOM) were removed by treating samples with hydrogen peroxide and leaching with distilled water, and D-sodium hexametaphosphate was used as a dispersing agent (Day, 1965). Soil temperature corrections were applied to ensure accurate readings (Elfaki et al., 2016).

Spectral data acquisition

In parallel, hyperspectral reflectance measurements were performed on the prepared soil samples in the hyperspectral remote sensing laboratory (National Authority for Remote Sensing and Space Sciences (NARSS), Egypt. However, each of the 140 soil samples was analyzed in laboratory conditions using a spectroradiometer in the visible to near-infrared (vis-NIR) spectral range from 350 nm to 2500 nm, with data collected at 1 nm intervals (figure 3). Each sample was placed in a circular glass petri dish, as illustrated in the referenced methodology. The ASD FieldSpec spectroradiometer (Boulder, CO) was employed to measure the reflectance of each soil sample. The sensor was positioned at nadir, with an optic angle of 18°, and the distance from the optic to the sample background was set at 65 cm, resulting in an instantaneous field of view of 21.1 cm. This setup followed the procedures described by Streck et al. (2003) and Liu et al. (2020).

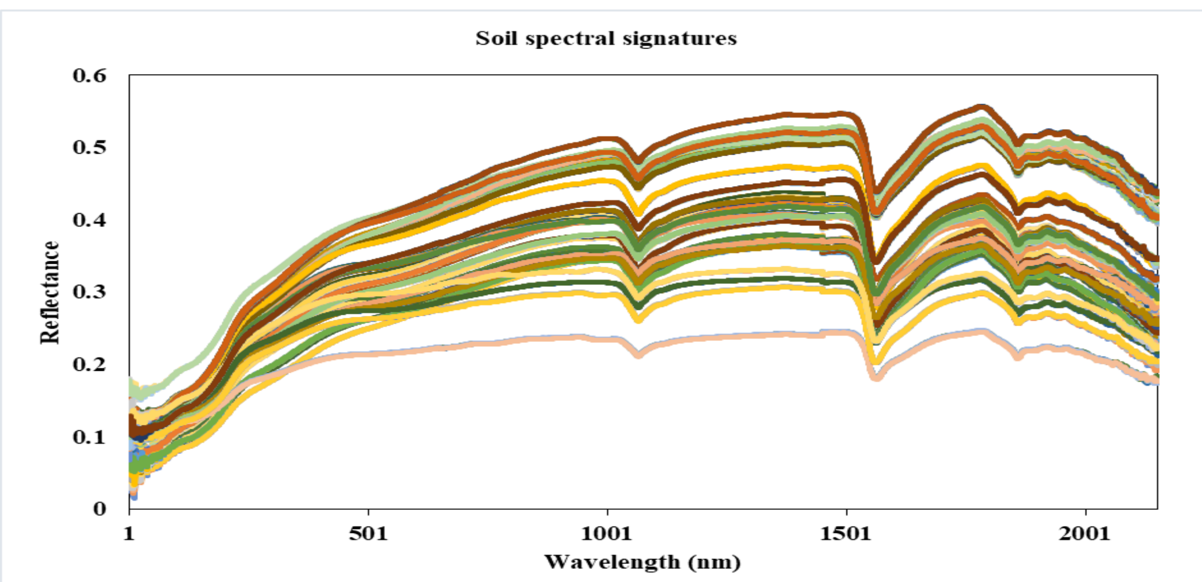

Figure (3). Soil spectral signatures in the spectral range 350-2500nm.

Mathematical and statistical analyses

The descriptive statistical analysis of the obtained data of the soil wet-chemistry analysis was done using the MS-Excel tools whereas the values of mean, minimum, maximum, standard error, standard deviation, sample variance, and range was estimated for each soil property. Correlation between the soil properties was done using R software (R Core Team, 2024) to overview the relation among different properties. To investigate the relationships between soil properties and their spectral signatures, the EC, CEC, clay, and $CaCO_3$ values were statistically correlated with the corresponding spectral data using R software.

Correlation analysis between soil properties and spectral data

To investigate the relationships between measured soil properties and spectral reflectance data, a correlation analysis was performed using the R statistical environment (R Core Team, 2024). The input dataset was organized as a comma-separated values (CSV) file, with the first column containing the target soil property (e.g., calcium carbonate content, CEC, clay, or EC) and the subsequent columns containing spectral reflectance values at different wavelengths for each soil sample. The analysis proceeded as first, the CSV file was imported into R, and the soil property values were extracted from the first column. Spectral data columns were then converted to numeric values to ensure compatibility and to address any potential formatting inconsistencies. For each spectral band (i.e., each wavelength column), the Pearson correlation coefficient was calculated between the soil property values and the corresponding spectral reflectance values across all samples, using the cor() function with the complete.obs option to handle any missing data. The resulting correlation coefficients were paired with their respective wavelengths, and the output was saved as a new CSV file for further interpretation. To visualize the correlation patterns across the spectral range, a correlogram was generated using the ggplot2 package in R. This plot displays the correlation coefficient as a function of wavelength, highlighting spectral regions most sensitive to the soil property of interest. The correlogram was exported as a high-resolution JPEG image for inclusion in the results. This approach enabled efficient identification of key spectral bands associated with specific soil properties, providing a robust foundation for subsequent predictive modeling and interpretation.

RESULT AND DISCUSSION

Soil characterization

Table (1) showed the descriptive statistical analysis of the investigated soil properties. The soil $CaCO_3$ content ranged from 0.76 to 34.60% with an average of 5.82%; and these soils varied between non-calcareous to calcareous according to (FAO, 2016). Moreover, the CEC of the investigated soils ranged from 1.44 to 32.38 cmol(+)/kg; and the average value was 9.22 cmol(+)/kg. Regarding the minimum, maximum, and average values of the clay parameter were 1.59, 54.76, and 16.79%, respectively. Furthermore, the ECe differed from 0.38 to 30.24 dS/m with an average of 4.82 dS/m in the studied soil samples; whereas the soils ranged from non-saline to strongly saline (USSL, 1954). From the obtained data, it is obvious that the highest standard error value was recorded for the clay parameter (0.86%), followed by the CEC (0.62 cmol(+)/kg); $CaCO_3$ (0.55%); and ECe (0.44 dS/m). The table also shows that the standard deviation value for each property was 6.48 for $CaCO_3$, 7.34 for soil CEC, 10.23 for clay percentage, and 5.22 for ECe. The corresponding table also showed that the sample variance values were large in some properties because the soil samples were collected from old and newly cultivated lands. The variance value of $CaCO_3$ was 41.98, for CEC was 53.85, of clay was 104.66, which is the highest; and was 27.22 for the soil ECe. This wide variance is attributed to the wide spatial variability between the soil samples which were collected from more than one site, including old and newly cultivated sites.

Table (1). Descriptive statistics of the examined soil properties.

Statistical parameter	$CaCO_3$	CEC	Clay	EC_e
	%	cmol($^+$)/kg	%	dS/m
Mean	5.82	9.22	16.79	4.82
Standard Error	0.55	0.62	0.86	0.44
Standard Deviation	6.48	7.34	10.23	5.22
Sample Variance	41.98	53.85	104.66	27.22
Range	33.84	30.94	53.17	29.86
Minimum	0.76	1.44	1.59	0.38
Maximum	34.60	32.38	54.76	30.24

There are considerable evidences to support the findings of current work such as the study conducted by Ibrahim et al. (2021) who found that the $CaCO_3$ content in the old cultivated soils of Sohag Governorate ranged between 0.31 and 10.30%. Additional support came from Moursy and Thabit (2022) who found that the $CaCO_3$ content in some desert soils of Sohag Governorate varied from 4.96 to 11.05%. Likewise, Mustafa (2023) observed that the $CaCO_3$content in the soils of Sohag Governorate ranged between 0.53 and 38.12%. Regarding to the CEC content in the soils of Sohag Governorate, many studies were conducted (i.e., Mustafa and Moursy, 2020; Ibrahim et al., 2021; Mustafa et al., 2024; Mustafa, 2023 and Shokr et al., 2024; and others). The previous studies revealed that the old cultivated soils had the highest values of CEC while the lowest were observed in the desert areas; and the moderate CEC content was recorded for the newly reclaimed soils. For instance, Mustafa (2023) found that the CEC content in the soils of Sohag Governorate varied from 1.73 to 18.05 cmol(+)/kg. Similarity, Mustafa et al., (2024) observed that the CEC content in the soils of Sohag Governorate ranged from 17.91 to 30.35 cmol(+)/kg. These findings are almost consistent with our laboratory observations of the wet chemistry testing. The clay content of the study area varied according to the land use and management practices. Accordingly, Ibrahim et al., (2021) found through laboratory analysis that the percentage of clay content in various soils of Sohag Governorate ranged between 1.04 and 60.80%. Similarly, Mustafa (2023) mentioned that clay varied from 2 to 48.95% in some of Sohag soils. Mustafa (2023) found that ECe values differed between 0.26 and 20.41 dS/m in some soils of Sohag; while Negim and Moursy (2023) ovserved that the ECe in various soils collected from three separate sites in Sohag Governorate ranged between 1.07 and 3.69 dS/m. Moreover, Mustafa and Moursy (2020) found that ECe varied from 0.26to 3.65 dS/m; while Moursy and Thabit (2022) found that the ECe ranged between 1.16 and 7.00 dS/m in some soils collected from Sohag. However, these results are in consistent with our laboratory analysis of the soil samples under study in Sohag Governorate.

Correlation between soil properties

The figure (4) presents a correlation matrix for the soil properties. The most notable positive correlation is between $CaCO_3$ and CEC (r = 0.52), suggesting that soils with higher calcium carbonate content tend to have higher cation exchange capacity. This relationship may be due to the influence of $CaCO_3$ on soil structure and its contribution to the overall cation exchange sites in calcareous soils. In contrast, $CaCO_3$ shows moderate negative correlations with both clay content (r = -0.25) and EC (r = -0.30). This indicates that as calcium carbonate increases, there is a tendency for clay content and soil salinity (as measured by EC) to decrease, which could be related to the dilution effect of $CaCO_3$ in sandy or less clay-rich soils, or to the leaching of salts in calcareous environments. CEC has weak negative correlations with both clay content (r = -0.18) and EC (r = -0.20), which is somewhat unexpected since clay minerals typically contribute to higher cation exchange capacity. This weak relationship may reflect the dominance of other soil factors, such as organic matter or mineralogy, or the influence of land management and reclamation practices in the sampled area. The only moderate positive correlation among the remaining pairs is between clay content and EC (r = 0.34), suggesting that soils with higher clay content tend to have higher electrical conductivity, possibly due to greater retention of salts and moisture in finer-textured soils.

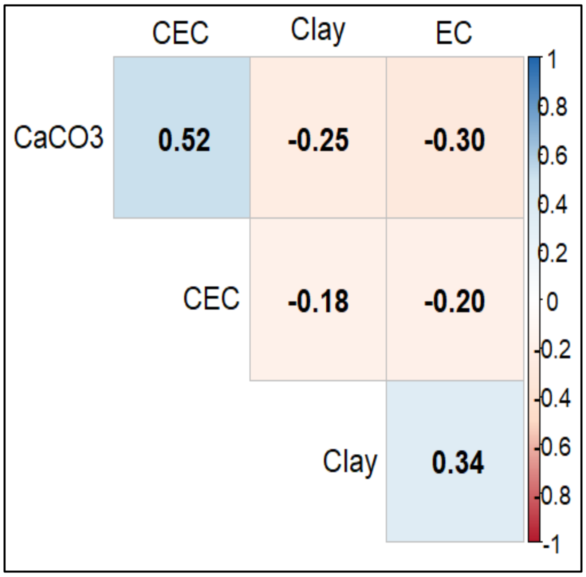

Figure (4). Correlation matrix of the soil properties.

Soil spectral data

It is very important to understand the spectral signature behavior of soil to determine the interaction between spectra, reflectance, and different soil parameters. It is evident that there is variation in reflectance values among soil samples. This variation is due to the variation in color, chemical structure, texture, consistency, compaction, SOM content, mineral composition, iron oxides, and other internal factors. However, there are sharp peaks observed at wavelengths of 1400, 1900, and 2200 nm due to strong spectral absorption of O-H hydroxyl functional groups (Chauhan et al., 2021). Vis-NIR spectral data typically exhibits specific absorption and reflectance patterns that are indicative of material composition, allowing for the identification of key characteristics such as moisture content, SOM, nutrient levels, and other relevant parameters (Bai et al., 2022). The spectral behavior of soil $CaCO_3$ (figure 5a) shows that as $CaCO_3$ content increases, soil reflectance also rises, with samples high in $CaCO_3$ exhibiting the greatest reflectivity. This is consistent with the principle that lighter-colored materials reflect more light than darker ones (Ben-Dor et al., 1999). Previous studies, including Lagacherie et al. (2008), Mitran et al. (2021), Qi et al. (2021), Shahabi et al. (2023), and Shokr et al. (2024), confirm that soils with higher $CaCO_3$ content display higher reflectance and lower absorption. For CEC (figure 5b), the spectral data reveal that soils with lower CEC have higher reflectance, while those with higher CEC show reduced reflectivity. This pattern is attributed to the increased nutrient retention in soils with higher CEC, which affects their optical properties and results in darker appearance and greater absorption (Ben-Dor et al., 1999; Milos et al., 2022). Similar findings by Mustafa et al. (2024) and Shokr et al. (2024) demonstrate that increasing CEC leads to decreased reflectance and increased absorption.
Regarding clay content (figure 5c), the spectra indicate that as clay percentage increases, reflectance decreases and absorption increases. Soils with the highest clay content have the lowest reflectivity, while those with the least clay have the highest reflectivity, again reflecting the general principle that darker, finer-textured soils absorb more light (Ben-Dor et al., 1999). This trend is supported by studies from Wang et al. (2021), Mitran et al. (2021), and Bellinaso et al. (2021), all of which report that higher clay content results in reduced soil reflectance. For ECe (figure 5d), the spectral data show that higher soil salinity is associated with increased reflectance and decreased absorption. This relationship, observed in Figure 18, is consistent with the findings of Nawar et al. (2015), Medhat et al. (2021), Abdellatif et al. (2021), and Wang et al. (2023), who also found that as soil ECe increases, reflectivity rises and absorption diminishes, in line with established theories of light reflection in soils.

Correlograms of the different soil properties

(a) Calcium Carbonate ($CaCO_3$)

The correlogram (Figure 6a) shows the correlation between spectral reflectance and $CaCO_3$ content across the soil samples. The plot reveals a strong negative correlation particularly in the 2200–2350 nm range, with correlation coefficients dropping below –0.60 in some bands. This wavelength region is well-known for featuring carbonate absorption bands, especially due to the combination and overtone vibrations of CO_3 groups. The negative correlation implies that higher $CaCO_3$ content is associated with lower reflectance (darker pixels) in those spectral regions, possibly due to enhanced absorption by carbonate minerals. A secondary region of interest is between 1900–2000 nm, where moderate correlations are also visible, potentially related to overlapping water bands or indirect effects of carbonate on soil moisture retention.

(b) Cation Exchange Capacity (CEC)

Correlogram (Figure 6b) reflects the relationship between spectral data and CEC values. The observed correlations are positive, with maximum peaks in the 2100–2250 nm range, reaching values close to +0.60. These wavelengths are typically influenced by clay minerals, especially smectites and illites, which strongly contribute to CEC. A positive correlation in this region suggests that soils with higher reflectance (i.e., lighter tone) correspond to higher CEC values, possibly because high CEC clays like smectites also reflect more light in those wavelengths. This association is often strengthened by the presence of OH and Al–OH combinations, which dominate absorption in this part of the SWIR region.

(c) Clay Content

In correlogram (Figure 6c), clay content exhibits strong positive correlations, again primarily within the 2100–2300 nm range, with values peaking beyond +0.70. These wavelengths are consistent with the diagnostic absorption features of clay minerals due to Al–OH and Mg–OH bonds. Lesser, but still relevant, correlations may also appear around 1400 and 1900 nm, indicating moisture-related absorption possibly influenced by clay's water-holding capacity. The positive nature of the correlation implies that higher clay content leads to increased reflectance in these regions, likely due to internal scattering from fine-textured surfaces. The magnitude and specificity of the correlations reflect the strong and consistent spectral expression of clay minerals.

(d) Electrical Conductivity (EC)

Correlogram (Figure 6d) illustrates the relationship between EC and spectral reflectance. The correlation trend here is somewhat more complex and moderate, but noticeable positive correlations emerge around 1450 nm, 1950 nm, and weakly near 2200–2300 nm, though with lower strength (approximately +0.40 to +0.50). These regions align with moisture and salt-associated features, suggesting indirect detection of salinity. Salinity affects reflectance indirectly by altering moisture retention and causing salt crust formation, which can brighten or darken soil surfaces depending on the salt types. The positive correlations suggest higher EC values are associated with higher reflectance, potentially due to salt accumulation on the soil surface increasing brightness.

General insights and applications

The consistent presence of significant correlations in the SWIR region (1900–2350 nm) across all four properties highlights its critical role in soil property estimation. These findings reinforce the importance of selecting appropriate wavelength bands for model calibration, especially in soil spectral libraries and digital soil mapping applications. Moreover, the ability to detect multiple properties using overlapping spectral regions supports the feasibility of multi-target predictive modeling, improving the efficiency of soil monitoring programs. These correlograms also validate the quality of the collected spectral data, showing that the reflectance measurements capture real and interpretable signals linked to soil composition. In a broader sense, such spectral–property relationships pave the way for non-destructive, rapid, and cost-effective soil analysis methods, which are essential for sustainable land management, precision agriculture, and large-scale soil surveys.

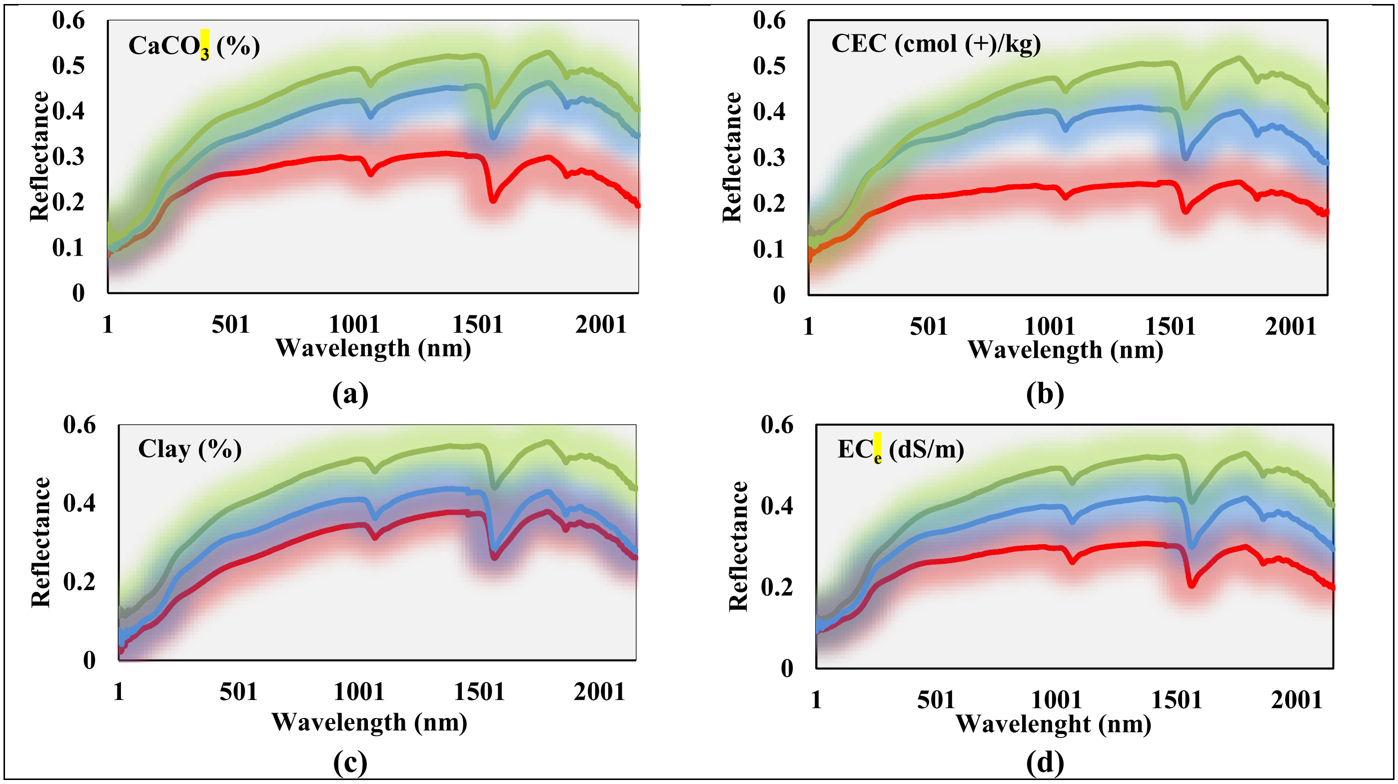

Figure (5). Spectral signatures' behaviors of the soil properties: (a) CaCO3; (b) CEC; (c) Clay; and (d) EC.

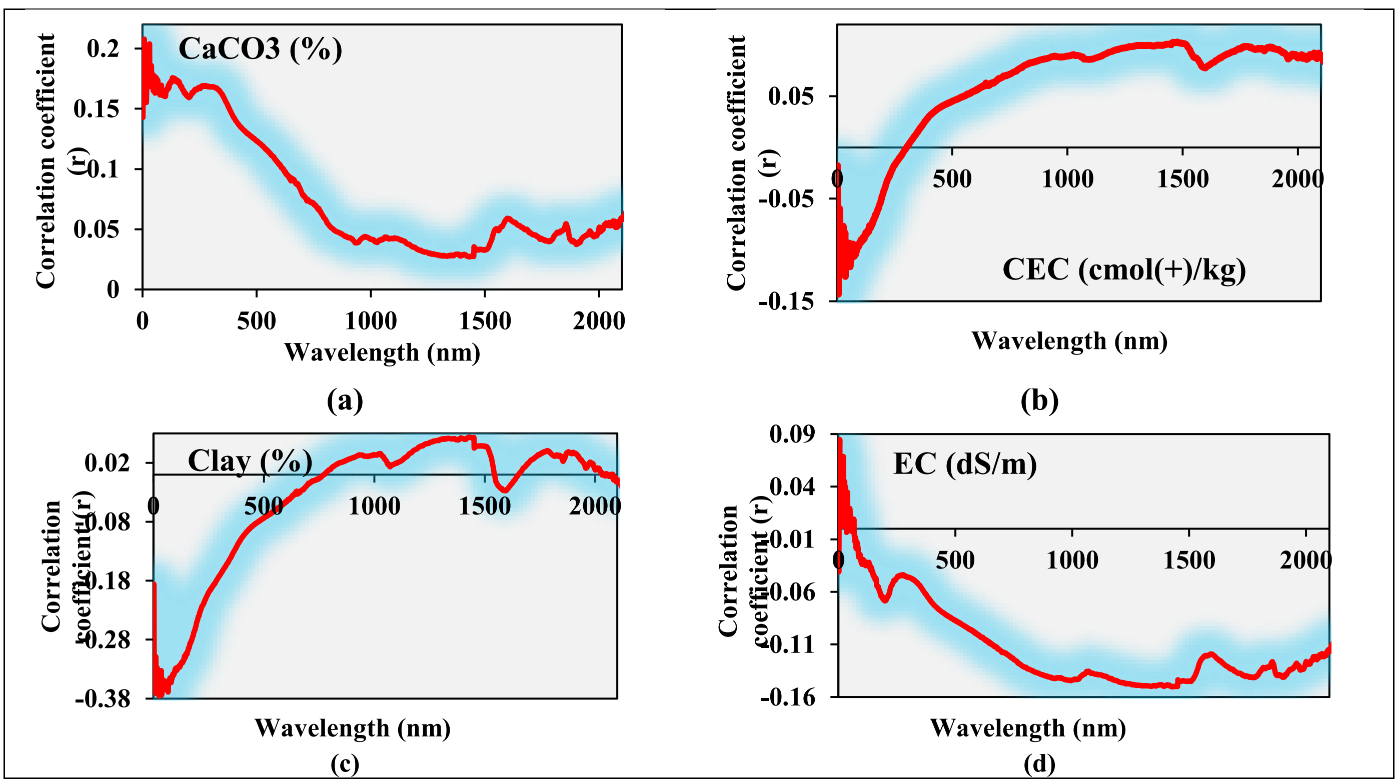

Figure (6). Correlograms of different soil properties against the spectral data; (a) CaCO3; (b) CEC; (c) Clay; and (d) EC.

Comparison between the two approaches used for soil characterization

The comparison between conventional laboratory methods and vis-NIR spectral techniques for soil characterization in the Sohag Governorate revealed notable distinctions in terms of accuracy, efficiency, and practicality. Traditional wet-chemistry methods involved precise but labor-intensive procedures, including volumetric determination of $CaCO_3$, hydrometer-based particle size analysis for clay, and titration for CEC. These methods provided highly accurate and validated data for the 140 collected samples, offering a detailed understanding of soil properties such as $CaCO_3$ (0.76–34.60%, mean 5.82%), CEC (1.44–32.38 cmol(+)/kg, mean 9.22), clay (1.59–54.76%, mean 16.79%), and EC (0.38–30.24 dS/m, mean 4.82). However, these analyses required extensive sample handling, chemical reagents, and processing time, making them less suitable for rapid or large-scale soil assessments. In contrast, the spectral method demonstrated substantial advantages in terms of speed, cost-effectiveness, and environmental sustainability. By acquiring vis-NIR reflectance data in the 350–2500 nm range, the study identified specific spectral regions that strongly correlated with key soil properties, such as 2200–2350 nm for $CaCO_3$ ($r < –0.60$), 2100–2300 nm for clay ($r > +0.70$), and 2100–2250 nm for CEC ($r \approx +0.60$). This method enabled rapid, non-destructive assessment of multiple soil parameters simultaneously and proved particularly useful in capturing the compositional diversity across old and newly reclaimed lands. However, its effectiveness relies heavily on robust calibration with reference laboratory data. Overall, while conventional methods remain essential for accurate baseline measurements and model development, vis-NIR spectroscopy offers a scalable and efficient alternative for ongoing soil monitoring and mapping across large areas.

CONCLUSION

The present study successfully characterized the spatial variability of key soil properties in Sohag Governorate, Egypt, using both conventional laboratory methods and visible to near-infrared (vis-NIR) spectroscopy. Laboratory analysis of 140 surface soil samples revealed wide ranges in soil attributes: calcium carbonate ($CaCO_3$) content varied from 0.76% to 34.60%, cation exchange capacity (CEC) ranged from 1.44 to 32.38 cmol(+)/kg, clay content spanned 1.59% to 54.76%, and electrical conductivity (ECe) extended from 0.38 to 30.24 dS/m. High variances, particularly in clay (104.66) and CEC (53.85), highlighted the impact of diverse land uses and reclamation stages. Vis-NIR spectral data (350–2500 nm) provided valuable insight into the spectral behavior of these soil properties. Strong negative correlations between $CaCO_3$ and reflectance were observed in the 2200–2350 nm region ($r < –0.60$), while CEC and clay content showed strong positive correlations ($r > +0.60$ and $+0.70$, respectively) in the 2100–2300 nm region. EC exhibited moderate positive correlations ($r \approx +0.40$ to $+0.50$) near 1450, 1950, and 2200 nm. These findings confirm that reflectance data, particularly in the shortwave infrared range, can serve as reliable proxies for estimating various soil properties, provided proper calibration against laboratory values. Based on these results, the study recommends adopting a hybrid approach that integrates vis-NIR spectral techniques with traditional wet-chemistry methods. While laboratory testing remains essential for calibration and validation, spectral data significantly reduce time, cost, and environmental impact when applied at scale. This integrated methodology is especially useful for soil surveys, digital soil mapping, and precision agriculture initiatives in arid and semi-arid regions like Sohag. For future work, it is recommended to develop and validate predictive models (e.g., PLSR or machine learning approaches) using the identified sensitive spectral bands. Additionally, extending the study to include organic matter, micronutrients, and soil moisture would broaden its applicability. Incorporating geostatistical and remote sensing tools, such as satellite hyperspectral imagery, could further enhance the spatial resolution and scalability of soil property mapping. Ultimately, this work contributes to building robust soil spectral libraries and supports sustainable land and crop management strategies.

REFERENCES

Abd-Elazem, A. H., El-Sayed, M. A., Fadl, M. E., Zekari, M., Selmy, S. A., Drosos, M., ... & Moursy, A. R. (2024). Estimating Soil Erodible Fraction Using Multivariate Regression and Proximal Sensing Data in Arid Lands, South Egypt. Soil Systems, 8(2), 48.

Abdellatif, A. D., Abou-Kota, M. E. S., Ganzour, S. K., & Allam, A. S. (2021). Soil spectral reflectance behavior related to chemical soil properties and macronutrients using the PLSR model. International Journal of Agricultural & Statistical Sciences, 17(1).

AbdelRahman, M. A., Metwaly, M. M., Yossif, T. M., & Moursy, A. R. (2025). Using hyperspectral data to estimate and map surface and subsurface soil salinity, pH, and calcium carbonates in arid region. Environmental Sustainability, 1-21.

Ahmed, A. A. (2007). Using lithologic modeling techniques for aquifer characterization and groundwater flow modeling of Sohag area, Egypt. Second International Conference on Geo-Resources in The Middle East and North Africa, 24–28 Feb, 2007, Cairo University, Egypt.

Ahmed, A., & Ali, M. (2011). Hydrochemical evolution and variation of groundwater and its environmental impact at Sohag, Egypt. Arabian Journal of Geosciences, 4.

Bai, Z., Xie, M., Hu, B., Luo, D., Wan, C., Peng, J., and Shi, Z. (2022). Estimation of soil organic carbon using vis-nir spectral data and spectral feature bands selection in southern Xinjiang, China. Sensors, 22(16), 6124.

Baruah, T.C. & Barthakur, H.P. (1997). A textbook on Soil Analysis. Vikas Publishing House PVT LTD, 576 Masjid Road, Jangpura, New Delhi 110 014.

Bellinaso, H., Silvero, N. E., Ruiz, L. F. C., Amorim, M. T. A., Rosin, N. A., de Sousa Mendes, W., ... & Dematte, J. A. (2021). Clay content prediction using spectra data collected from the ground to space platforms in a smallholder tropical area. Geoderma, 399, 115116.

Ben-Dor, E., Irons, J. R., & Epema, G. F. (1999). Soil reflectance. Remote sensing for the earth sciences: Manual of remote sensing, 3(3), 111-188.

CAPMAS (Central Agency for Public Mobilization and Statistics) (2025), Egypt.

Chauhan, R., Kumar, R., Kumar, V., Sharma, K., & Sharma, V. (2021). On the discrimination of soil samples by derivative diffuse reflectance UV–vis-NIR spectroscopy and chemometric methods. Forensic science international, 319, 110655.

Day, P. R. (1965). Particle Fractionation and Particle-Size Analysis. In C. A. Black (ed) Methods of Soil Analysis. Part I. Soil Sci. Soc. Amer.

Elfaki, J. T., Gafer, M. A., Sulieman, M. M., & Ali, M. E. (2016). Hydrometer method against pipette method for estimating soil particle size distribution in some soil types selected from Central Sudan. International Journal of Engineering Research and Advanced Technology, 2(2), 25-41.

El-Sayed, M. A., Abd-Elazem, A. H., Moursy, A. R., Mohamed, E. S., Kucher, D. E., & Fadl, M. E. (2023). Integration vis-NIR spectroscopy and artificial intelligence to predict some soil parameters in arid region: A case study of Wadi Elkobaneyya, South Egypt. Agronomy, 13(3), 935.

El-Sayed, M. A., Faragallah, M. A., El-Desoky, A. I., & Fadl, M. E. (2020). Geostatistical models for land capability evaluation of Wadi Tag El-Wabar, Sohag, Egypt. Archives of Agriculture Sciences Journal, 3(2), 94-106.

El-Zohry, M. A., El-Zayat, M. H., Hassaneen, K. S., Mahmoud, A. A., Tawik, S. T., & Abdellah, W. M. (2024). Assessment of Natural Radionuclide Concentrations (238U, 232Th, and 40K) in Soil Samples from Different Locations in Sohag Governorate, Egypt. Sohag Journal of Sciences, 9(1), 99-104.

Embaby, A., Ali, M. H., & Saber, E. A. (2023). Groundwater Suitability Assessment in Western Sohag Governorate, Upper Egypt. Frontiers in Scientific Research and Technology, 7(1).

FAO. (2016). FAO Soils Portal: Management of Calcareous Soils.

General Authority for Inquiries, Egypt, 2023.

Ibrahim, M. S., Hassan, M., & Osman, H. (2021). The cultivation period effects on heavy metals content of some soils of Sohag governorate. Journal of Sohag Agriscience (JSAS), 6(2), 124-136.

Jackson, M.L. 1973. Soil chemical analysis. Prentice-Hall, Inc., Engle wood Cliffs. NJ, USA.

Lagacherie, P., Baret, F., Feret, J. B., Netto, J. M., & Robbez-Masson, J. M. (2008). Estimation of soil clay and calcium carbonate using laboratory, field and airborne hyperspectral measurements. Remote Sensing of Environment, 112(3), 825-835.

Liu, Y., Deng, C., Lu, Y., Shen, Q., Zhao, H., Tao, Y., and Pan, X. (2020). Evaluating the characteristics of soil vis-NIR spectra after the removal of moisture effect using external parameter orthogonalization. Geoderma, 376, 114568.

Medhat Saleh, A., Abd-Elwahed, M., Metwally, Y., & Arafat, S. (2021). Capabilities of Hyperspectral Remote Sensing Data to Detect Soil Salinity. Arab Universities Journal of Agricultural Sciences, 29(3), 943-952.

Miloš, B., Bensa, A., & Japundžić-Palenkić, B. (2022). Evaluation of Vis-NIR preprocessing combined with PLS regression for estimation soil organic carbon, cation exchange capacity and clay from eastern Croatia. Geoderma regional, 30, e00558.

Mitran, T., Sreenivas, K., Janakirama Suresh, K. G., Sujatha, G., & Ravisankar, T. (2021). Spatial prediction of calcium carbonate and clay content in soils using airborne hyperspectral data. Journal of the Indian Society of Remote Sensing, 49(11), 2611-2622.

Mitran, T., Sreenivas, K., Janakirama Suresh, K. G., Sujatha, G., & Ravisankar, T. (2021). Spatial prediction of calcium carbonate and clay content in soils using airborne hyperspectral data. Journal of the Indian Society of Remote Sensing, 49(11), 2611-2622.

Mondal, B. P., Sahoo, R. N., Das, B., Ahmed, N., Bandyopadhyay, K. K., Mukherjee, J., Arora, A., & Moursy, A. R. A. (2025). Comparison of multivariate machine learning models for major soil nutrients prediction using laboratory-based and airborne (AVIRIS-NG) visible near-infrared spectroscopy. European Journal of Agronomy, 170, 127726.

Mondal, B. P., Sekhon, B. S., Banerjee, K., Sharma, S., Setia, R. K., Das, B., ... & Moursy, A. R. (2024). Spatial variability of soil microbiological properties under different land use systems. African Journal of Agricultural Research, 20(9), 825-839.

Moursy, A. R. (2025). Hyperspectral Remote Sensing as an Alternative to Conventional Methods of Soil Analysis. In Smart Technologies in Sustainable Agriculture (pp. 221-254). Apple Academic Press.

Moursy, A. R., & Thabit, F. N. (2022). Soil Characterization and Estimation of the Current and Future Productivity of the Faculty of Agriculture Farm, Sohag University, Egypt. Journal of Soil Sciences and Agricultural Engineering, 13(9), 295-302.

Moursy, A. R., El-Galil, A. A., Ibrahim, M. S., El-Hady, A. A., & Mhalla, B. (2020). Characterization and classification of soils of Wadi Qena, Eastern Desert, Egypt.

Moursy, A. R., Elsayed, M. A., Fadl, M. E., & Abdalazem, A. H. (2025). PRISMA-Driven Hyperspectral Analysis for Characterization of Soil Salinity Patterns in Sohag, Egypt. Egyptian Journal of Soil Science, 65(1).

Moursy, A. R., Hassan, M. N., & Elhefny, T. M. (2022). Sampling and analysis of soil and water: A review. Int. J. Geogr. Geol. Environ, 4, 34-41.

Mustafa, A. A. (2023). Incorporate the Fertility Capability Classification and Geo-informatics for Assessing Soil: A Case Study on Some Soils of Sohag Governorate, Egypt. Journal of Soil Sciences and Agricultural Engineering, 14(7), 187-193.

Mustafa, A. E. R. A., & Moursy, A. R. (2020a). Integration of geoinformatics and ahp model for soil site suitability analysis for the major crops in Sohag, Egypt. International Journal of Recent Advances in Multidisciplinary Research, 7(7), 5784-5796.

Mustafa, A. E. R. A., & Moursy, A. R. (2020b). Using a multivariate regression model and hyperspectral reflectance data to predict soil parameters of Agra, India. International

Journal of Geography, Geology and Environment, 2(1), 4-9.

Mustafa, A. R. A., & Moursy, A. R. (2022). Efficiency of Geostatistical Analysis and Kriging for Predicting Soil Available NPK in El-Kawthar Region, Sohag, Egypt. In International Conference of Remote Sensing and Space Sciences Applications (pp. 269-279). Cham: Springer Nature Switzerland.

Nawar, S., Buddenbaum, H., & Hill, J. (2015). Estimation of soil salinity using three quantitative methods based on visible and near-infrared reflectance spectroscopy: a case study from Egypt. Arabian Journal of Geosciences, 8, 5127-5140.

Negim, O. I., & Moursy, A. R. A. (2023). Effect of Long-Term Irrigation with Sewage Wastewater on Land Capability of Three Sites in Sohag Governorate, Egypt. Journal of Soil Sciences and Agricultural Engineering, 14(8), 235-246.

Negim, O., & Mustafa, A. (2016). Remediation of a highly calcareous saline sodic soil using some soil amendments. International Journal of Physical and Social Sciences, 12(5), 1-13.

Nungula, E. Z., Mugwe, J., Massawe, B. H., & Gitari, H. I. (2024). Morphological, pedological and chemical characterization and classification of soils in Morogoro District, Tanzania. Agricultural Research, 13(2), 266-276.

Ouda, S. A., Zohry, A. E. H., Zohry, A. E. H., & Ouda, S. A. (2016). Upper Egypt: management of high-water consumption crops by intensification. Management of climate induced drought and water scarcity in Egypt: Unconventional solutions, 63-76.

Qi, Y., Qie, X., Qin, Q., & Shukla, M. K. (2021). Prediction of soil calcium carbonate with soil visible-near-infrared reflection (Vis-NIR) spectral in Shaanxi province, China: Soil groups vs. spectral groups. International Journal of Remote Sensing, 42(7), 2502-2516.

R Core Team. (2024). R: A language and environment for statistical computing. R Foundation for Statistical Computing, Vienna, Austria. https://www.R-project.org/

Shahabi, A., Davari, M., Nabiollahi, K., & Taghizadeh Mehrjardi, R. (2023). Evaluation of PLSR and bagging-PLSR methods in estimating soil texture, calcium carbonate, and pH using spectral data. Iranian Journal of Soil and Water Research, 54(8), 1215-1231.

Shokr, M. S., Mustafa, A. R. A., Alharbi, T., Meroño de Larriva, J. E., El-Sorogy, A. S., Al-Kahtany, K., & Abdelsamie, E. A. (2024). Integration of VIS–NIR Spectroscopy and Multivariate Technique for Soils Discrimination Under Different Land Management. Land, 13(12), 2056.

Streck, N. A., Rundquist, D., & Connot, J. (2003). Spectral signature of selected soils. Rev. Brasil. Agrometeorol., Santa Maria, 11(1), 184.

Thabit, F. N., & Moursy, A. R. (2024). Sensors' Efficiency in Smart Management of the Environmental Resources. In Handbook of nanosensors: Materials and technological applications (pp. 1179-1218). Cham: Springer Nature Switzerland.

U.S. Salinity Laboratory (1954). Methods for soil characterization In Diagnosis and improvement of saline and alkali soils. USDA-Agricultural Handbook No. 60. U.S. Government Printing Office, Washington, D.C.

Wang, C., Qiao, X., Li, G., Feng, M., Xie, Y., Sun, H., Zhang, M., Song, X., Xiao, L., Anwar, S., & Yang, W. (2021). Hyperspectral estimation of soil organic matter and clay content in loess plateau of China. Agronomy Journal, 113(3), 2506-2523.

Wang, X., Zhang, M. W., Guo, Q., Yang, H. L., Wang, H. L., & Sun, X. L. (2023). Estimation of soil organic matter by in situ Vis-NIR spectroscopy using an automatically optimized hybrid model of convolutional neural network and long short-term memory network. Computers and Electronics in Agriculture, 214, 108350.

Wang, Y., Zou, B., Chai, L., Lin, Z., Feng, H., Tang, Y., ... & Zou, H. (2024). Monitoring of soil heavy metals based on hyperspectral remote sensing: A review. Earth-Science Reviews, 104814.